# Supporting Information

# One step space confined synthesis of $Mo_2C_{1-x}N_x$ solid solution with superconductivity

Zhuang Zhang, ‡[a b] Yuqiang Fang[a b], Dong Wang [a], Shaoning Zhang [a], Gang Mu [*d] and Fuqiang Huang[*abc]

[a] State Key Laboratory of High Performance Ceramics and Superfine Microstructure, Shanghai Institute of Ceramics, Chinese Academy of Sciences, Shanghai 200050, P. R. China

[b] Center of Materials Science and Optoelectronics Engineering，University of Chinese Academy of Sciences, Beijing 100049, China

[c] State Key Laboratory of Rare Earth Materials Chemistry and Applications, College of Chemistry and Molecular Engineering, Peking University, Beijing 100871, P.R. China

[d] State Key Laboratory of Functional Materials for Informatics, Shanghai Institute of Microsystem and Information Technology, Chinese Academy of Sciences, Shanghai 200050, China.

## Experimental Procedures

### Synthesis of samples

Solid solution molybdenum carbide $Mo_2C_{1-x}N_x$ samples in the composition range $0 \leq x \leq 0.57$ were synthesized by a one-step solid reaction method. Molybdenum powder, graphite carbon powder and $C_3N_4$ (prepared by decomposing melamine at 550 °C) were weighed and ground with the stoichiometry in $Mo_2C_{1-x}N_x$ ($x$ = 0, 0.02, 0.08, 0.17,0.22, 0.35, 0.57). Then they are vacuum-sealed in silica quartz tubes. They were then placed in a muffle furnace and incubated at 1273 K for 3000 min.

### Characterization of Structure

The crystal structure of the prepared samples was characterized by powder XRD. XRD data was obtained in a Panalytical diffractometer (model Empyrean) with detector PIXcel3D accessory using Cu-$K_{\alpha 1}$ (1.5406 Å) and Bragg-Brentano geometry. The diffraction patterns were acquired in the 2θ range between 30° and 80° with steps of 0.02° and acquisition time of 0.1 s. The lattice parameters analyses, patterns simulation, and refinement of the structures (Rietveld method) were performed using fullprof and public software adopting as reference the orthorhombic $Mo_2C$ phase crystallographic data reported in the literature.

### Measurement of Physical Properties

Magnetic and electrical characterization of those samples were carried out by using a Quantum Design system PPMS. The phenomenon of superconductivity was defined from resistance, magnetization and specific heat (SH) measurements. Resistance was measured by a four-probe method with an applied current 1 mA. Magnetization ($M$) measurements were performed with a vibrating sample magnetometer (VSM) system; a DC external field of 10 Oe with both zero- field cooling (ZFC) and field cooling (FC) modes in the temperature range from 3 to 10 K was applied. The hysteresis loops of $M$ versus applied magnetic field ($H$) were acquired at 3 K in the $-10$ kOe $\leq H \leq$ 10 kOe range. Moreover, we employed the thermal relaxation technique to perform the specific heat measurements.

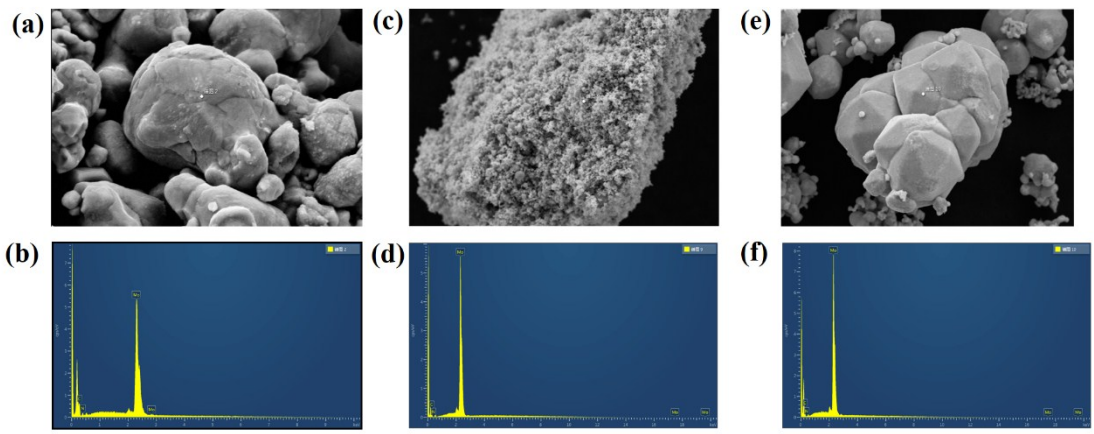


| Element | Line type | Atom % | Standard sample label |
|---|---|---|---|
| C | K | 35.50 | Pure Element |
| N | K | 18.05 | BN |
| Mo | L | 46.45 | Pure Element |

| Element | Line type | Atom % | Standard sample label |
|---|---|---|---|
| C | K | 56.19 | Pure Element |
| N | K | 0 | BN |
| Mo | L | 43.81 | Pure Element |

| Element | Line type | Atom % | Standard sample label |
|---|---|---|---|
| C | K | 57.50 | Pure Element |
| N | K | 0 | BN |
| Mo | L | 42.50 | Pure Element |

**Figure S1.** SEM images (a) and EDS analysis (b) of the sample prepared from Mo and $C_3N_4$ in confined system, SEM images (c) and EDS analysis (d) of the sample prepared from $Mo_2C$ and $NH_3$, SEM images (c) and EDS analysis (d) of the sample prepared from Mo, $CH_4$ and $NH_3$.

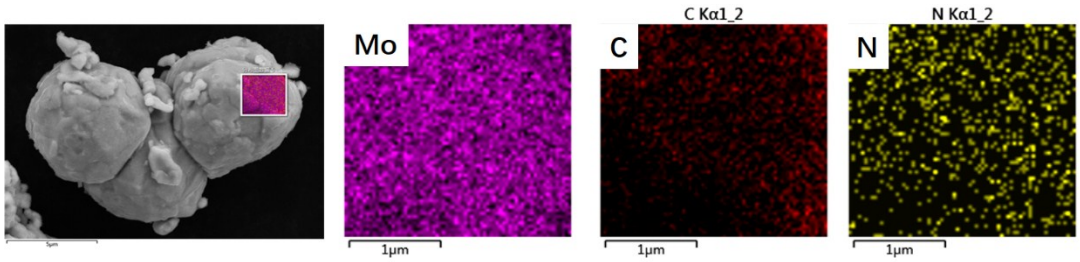


**Figure S2.** The EDS mapping of $Mo_2C_{0.43}N_{0.57}$.

**Table S1.** Theoretical and experimental values of nitrogen mass concentration in $Mo_2C_{1-x}N_x$.

| Chemical formula | Mass fraction of nitrogen (%) | |
|---|---|---|
| $Mo_2C_{1-x}N_x$ | theoretical | Experimental |
| $Mo_2C_{0.98}N_{0.02}$ | 0.14 | 0.18 |
| $Mo_2C_{0.92}N_{0.08}$ | 0.54 | 0.57 |
| $Mo_2C_{0.83}N_{0.17}$ | 1.16 | 1.14 |
| $Mo_2C_{0.78}N_{0.22}$ | 1.51 | 1.26 |
| $Mo_2C_{0.65}N_{0.35}$ | 2.39 | 1.92 |
| $Mo_2C_{0.43}N_{0.57}$ | 3.91 | 3.16 |

**Table S2.** From Rietveld refinement: lattice parameter, unit cell volume, R-factors ($R_{wp}$, $R_p$, and $R_e$) and goodness of fit ($S$) for each sample.

| N content (%) | Unit cell Parameters | | | | $R_p$ (%) | $R_{wp}$ (%) | $R_e$ (%) | $S$ |
|---|---|---|---|---|---|---|---|---|
| | $a$ (Å) | $b$ (Å) | $c$ (Å) | V (Å$^3$) | | | | |
| 0 | 4.7368 | 6.0323 | 5.2019 | 148.64 | 7.00 | 9.42 | 8.385 | 1.25 |
| 2 | 4.7372 | 6.0303 | 5.1998 | 148.54 | 7.03 | 9.28 | 8.433 | 1.21 |
| 8 | 4.7371 | 6.0237 | 5.1901 | 148.10 | 7.54 | 9.88 | 8.265 | 1.43 |
| 17 | 4.7416 | 6.0048 | 5.1863 | 147.67 | 8.05 | 10.4 | 8.271 | 1.59 |
| 22 | 4.7454 | 6.0186 | 5.1807 | 147.54 | 6.62 | 8.24 | 5.766 | 2.04 |
| 35 | 4.7519 | 5.9756 | 5.1693 | 146.79 | 8.97 | 11.99 | 8.583 | 1.95 |
| 57 | 4.7657 | 5.9518 | 5.1497 | 146.07 | 9.00 | 12.3 | 8.511 | 2.08 |

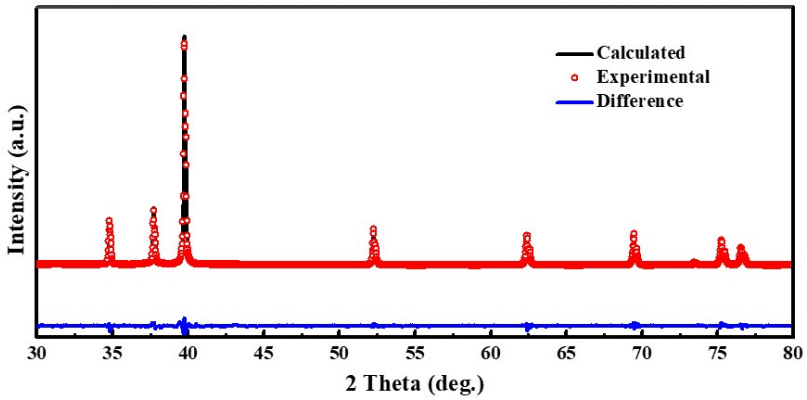


**Figure S3.** The fitting result of the XRD Rietveld refinement for the $Mo_2C_{0.43}N_{0.57}$ sample.

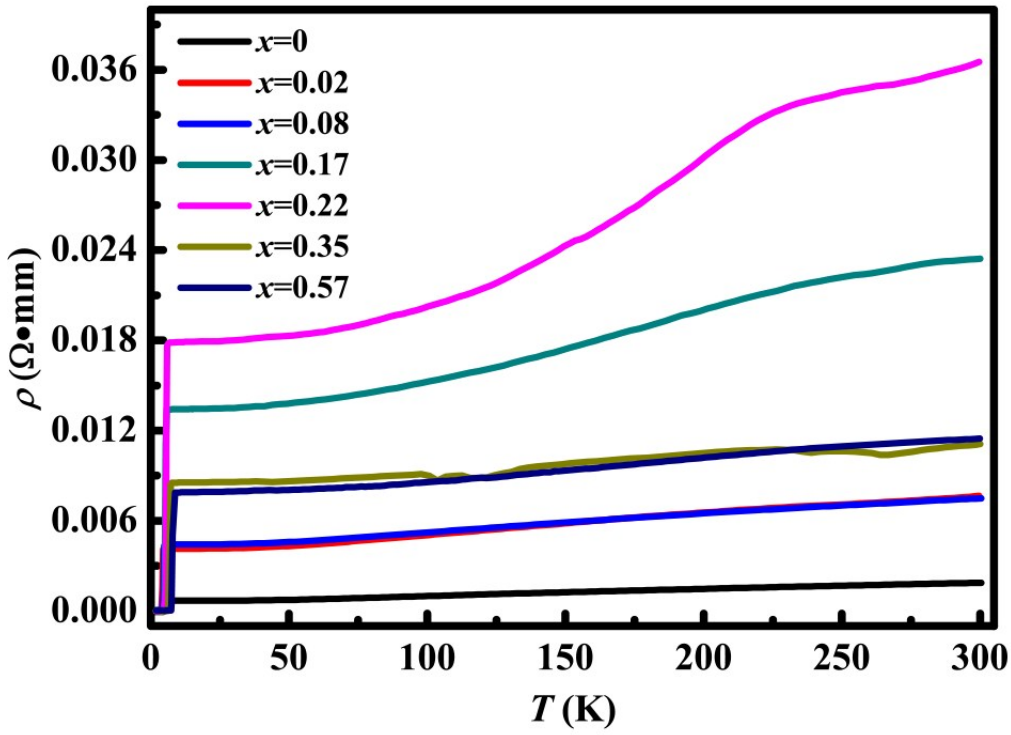


Figure S4. The resistivity of $Mo_2C_{1-x}N_x$ samples.

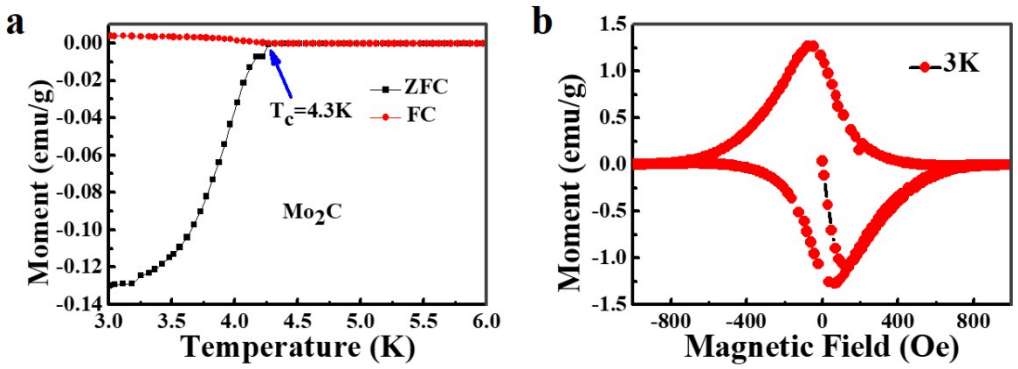


**Figure S5** (a) Temperature dependence of magnetic susceptibility of $Mo_2C$. (b) The magnetization loop of the $Mo_2C$ sample measured at 3 K.

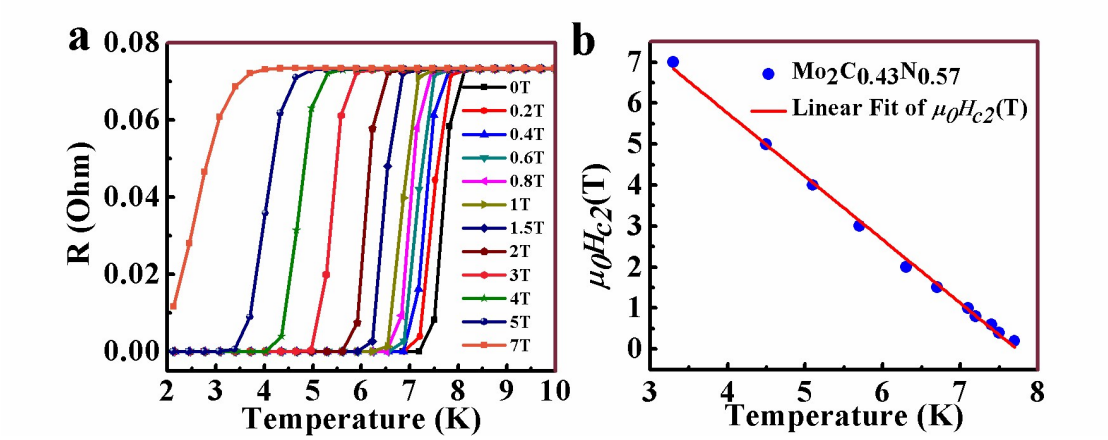


**Figure S6** (a) Electrical resistivity of $Mo_2C_{0.43}N_{0.57}$ measured under magnetic fields of 0, 0.2, 0.4, 0.6, 0.8, 1, 1.5 2.0, 3.0, 4.0, 5.0, 7.0T between 2 K and 10 K. (b) The relationship between temperature and upper critical magnetic field.

Superconducting behavior of the $Mo_2C_{1-x}N_x$ sample would be suppressed by magnetic field just like other superconductors, that can be used to calculate the upper critical field at zero Kelvin ($H_{2c}(0)$). The relationship between the resistance and temperature of the $Mo_2C_{0.47}N_{0.57}$ sample under different magnetic fields was measured in order to obtain the value of $H_{c2}(0)$ of $Mo_2C_{0.43}N_{0.57}$, which are shown in **Fig.S6a**. The corresponding values of $T_c$ are shown in **Fig.S6b**. The $H_{c2}(0)$ is estimated by using the Werthamer-Helfand-Hohenberg (WHH) theory: $H_{c2}(0) = -0.693 T_c \left(dH_{c2}/dT\right)_{T \to Tc}$ [25]. The slope of the line fitted to the data points in **Fig S6b** is $\left(dH_{c2}/dT\right)_{T \to Tc}$ = -1.51 T/K, and the $H_{c2}(0)$ of $Mo_2C_{0.43}N_{0.57}$ is calculated to be 8.3T. By the same method, the $H_{c2}(0)$ of $Mo_2C$ is calculated to be 7.48T.

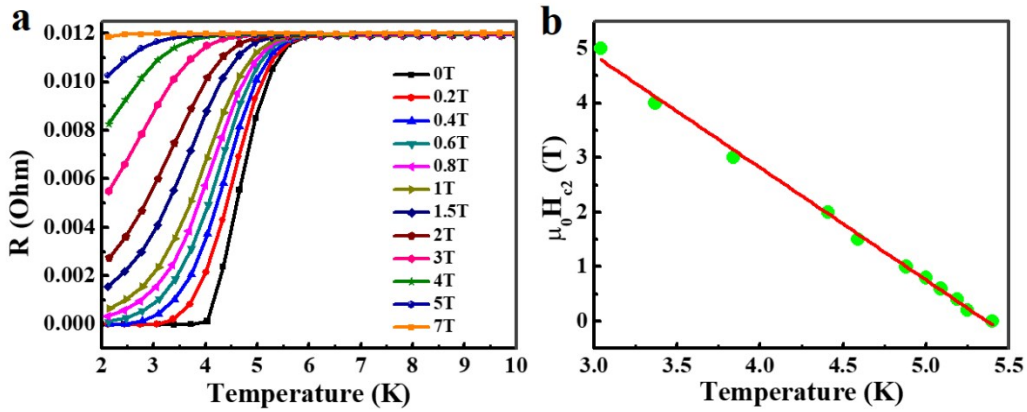


**Figure S7** (a) Electrical resistivity of $Mo_2C$ measured under magnetic fields of 0, 0.2, 0.4, 0.6, 0.8, 1, 1.5 2.0, 3.0, 4.0, 5.0, 7.0T between 2 K and 10 K. (b)The relationship between Temperature and upper critical magnetic field.

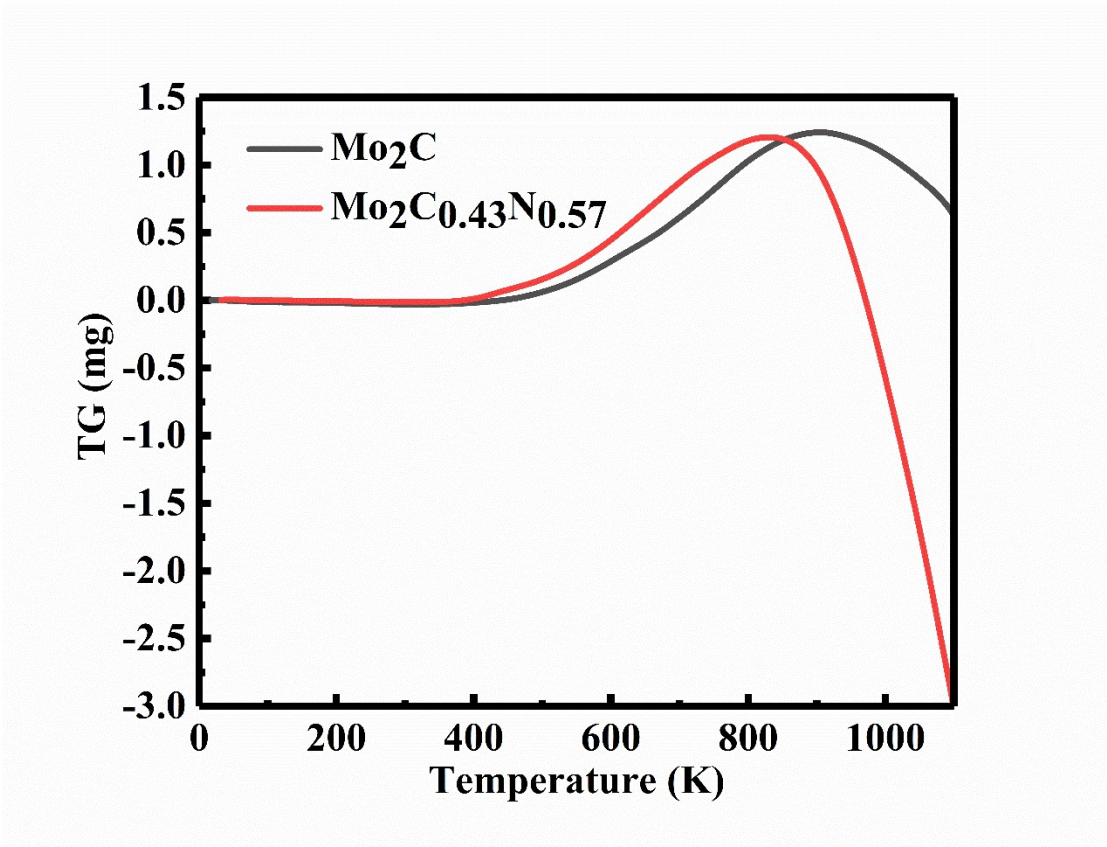


Figure S8 The thermal analysis data of $Mo_2C$ and $Mo_2C_{0.43}N_{0.57}$.

In the process of thermal analysis, air is mixed in the atmosphere because of the air tightness of the instrument. Therefore, $Mo_2C$ and $Mo_2C_{0.43}N_{0.57}$ began to oxidize at 400-500 ℃, and the sample mass increased. It can be seen from the figure that the temperature at which nitrogen-containing samples start to oxidize is lower, indicating that their stability in air is slightly worse than $Mo_2C$. The nitrogen-containing samples are very stable at room temperature.